Table 1 Comparison of shell thickness or penetration depth, meteoroid mass, and meteoroid density for various values of luminous efficiency and various penetration equations

$\bar{\tau}$	$\bar{t}$, $n = -\frac{1}{4}$	$\bar{t}$, $n = -\frac{1}{5}$	$\bar{p}$, $n = -\frac{1}{6}$	$\bar{m}$, $n = -1$	$\bar{\rho}$ $n = \frac{1}{2}$
0.1	1.78	1.58	1.47	10	0.32
1.0	1.0	1.0	1.0	1.0	1.0
10	0.56	0.63	0.68	0.1	3.2
100	0.32	0.40	0.47	0.01	10

$0.006 \leq m \leq 10.38$ g, and a multiwalled structure of 2024-T3 aluminum. Cour-Palais' relationship yields $t_b \propto \tau^{-1/4}$ for glass particles ($\rho = 2.3$ g/cm^3) for $7.5 \times 10^{-5} \leq m \leq 2.94 \times 10^{-3}$ gm impacting multilayer aluminum structures at between $5.4 \leq V \leq 6.7$ km/sec. For solid targets, Summers' relationship yields $p \propto \tau^{-1/6}$ for metal spheres with $1.5 \leq \rho \leq 17.1$ g/cm^3 fired into copper and lead targets at $0.16 \leq V \leq 3.6$ km/sec.

The uncertainties in m and ρ_m resulting from uncertainties in the value of τ are almost self-canceling when considering the meteoroid bumper penetration problem. This self-compensating effect was first noticed for single layer meteoroid shields by Whipple[6] and the same effect has been shown here to be true both for multi-wall and single-wall bumpers. Table 1 presents values for $\bar{t}$, $\bar{p}$, $\bar{m}$, and $\bar{\rho}$, which would result from variations in the values of τ over a range of three orders of magnitude. Here $\bar{\tau}$ is obtained by dividing τ by τ_{ref} (an arbitrary reference value of luminous efficiency). Likewise, $\bar{m} = (m/m_{\text{ref}})$, $\bar{\rho} = (\rho/\rho_{\text{ref}})$, $\bar{t} = (t/t_{\text{ref}})$, and $\bar{p} = (p/p_{\text{ref}})$ where m_{ref}, ρ_{ref}, t_{ref}, and p_{ref} are the m, ρ, t, and p resulting from calculations using the reference value of τ. In this table $\bar{t}$ or $\bar{p}$, $\bar{m}$ and $\bar{\rho}$ are expressed as function of τ^n.

Clearly, the meteoroid hazard is more severe than expected only if τ is significantly smaller than expected. McCrosky[7] discusses the possibility of increasing τ by a factor of 100 from an approximate value of 10^{-3} to make the luminous flux of large fireballs compatible with that from smaller meteors. This larger τ would reduce the expected meteoroid hazard from large objects by only from 53% to 68% depending upon the structure under consideration. As a practical example, Howard[5] has calculated for the Mars Mariner 71 mission a backup sheet thickness of 0.0081 cm will be required to survive an impact with a particle which has a d of 0.0792 cm, ρ of 0.5 g/cm^3, and a V of 20 km/sec. The actual shield as designed for this mission is 0.040 cm thick or 5 times as thick as required. This factor of 5 in thickness corresponds to allowing for uncertainty in the value of luminous efficiency. Using the equations relation τ and t or p in this Note, this extra shield thickness corresponds to a reduction by from 600 to 19,000 from the value of approximately 10^{-3} which is widely used for luminous efficiency.

For particles of a given V and τ, the required meteoroid bumper thickness t_s is shown to be a weak function of the luminous efficiency. Although the precise value of the luminous efficiency is uncertain, only a very large revision from its presently accepted value will significantly change the meteor bumper requirements.

References

[1] Whipple, F. L., "Meteors and the Earth's Upper Atmosphere," *Review of Modern Physics*, Vol. 15, 1943, pp. 246–264.

[2] Arenz, R. J., "Projectile Size and Density Effects on Hypervelocity Penetration," *Journal of Spacecraft and Rockets*, Vol. 6, No. 11, Nov. 1969, pp. 1319–1321.

[3] Cour-Palais, B. G., "Meteoroid Protection by Multiwall Structures," AIAA Paper 69-372, Cincinnati, Ohio, 1969.

[4] Summers, J. L., "Investigation of High Speed Impact: Regions of Impact and Impact at Oblique Angles," TN D-94, 1959, NASA.

[5] Howard, J. R., "Development of the Mariner Mars 1971 Meteoroid Shield," *Journal of Spacecraft and Rockets*, Vol. 7, No. 1, Jan. 1970, pp. 69–72.

[6] Whipple, F. L., "On Meteoroids and Penetration," *Journal of Geophysical Research*, Vol. 68, No. 17, Sept. 1963, p. 4929.

[7] McCrosky, R. E. and Ceplecha, Z., "Photographic Networks for Fireballs," Special Report 288, Oct. 1968, Smithsonian Astrophysical Observatory.

Optimization of Multistage Rockets Including Drag

CHARLES N. ADKINS*
Falls Church, Va.

Nomenclature

weight = value at sea level
B_j = ballistic coefficient at ignition of jth stage $= W_{ji}/S_j$
b_j, d_j = dimensionless similarity parameters, Eqs. (26) and (27)
C_D = drag coefficient
C_j = an average exhaust gas velocity, Eq. (16)
$\bar{C}_j$ = a generalized exhaust gas velocity, Eq. (26)
D_j = dimensionless similarity parameter $= 1 + R_j\bar{\beta}_j$
F = thrust
G, J = known functions of time, subscript j for burnout, Eq. (3)
$\bar{G}_j$ = similarity parameter, Table 1
g = acceleration due to gravity; g_0 at sea level
$\bar{g}_j$ = an average parameter, Eq. (16)
h_j = dimensionless similarity parameter, $= 1 + R_j\bar{Q}_j$
I = specific impulse, subscript j for burnout
k_j = average motor wall thickness per unit diameter
L_m = dimensionless similarity parameter, Eq. (29)
N_j = integral of G over burning time, Eq. (5)
n = total number of stages
p = payload; $p_j = W_{(j+1)i}$; p_n = final payload $= W_{1i}\prod_{j=1}^{n}\beta_j$
Q_j = a trajectory constant, Eq. (6)
$\bar{Q}_j$ = dimensionless similarity parameter, Eqs. (19) and (20)
q = dynamic pressure
R_j = ratio of propellant to inert motor weight $= \lambda_j/(1 - \lambda_j)$
$\dot{r}_j$ = burning rate, length per second
S = reference area for drag (cross section)
T_j = burning time for jth stage $= t_{jb} - t_{ji}$
t = time
U = the dimensionless compatibility function
u_j = a generalized dimensionless velocity increment
$V, \dot{V}$ = velocity and acceleration at time t
V_t = total velocity increment $= \sum_{j=1}^{n} v_j$
v_j = velocity increment for jth stage
W = vehicle weight at time t
x_j = parameter for end-burning stoges, Eq. (18)
α = angle between thrust and velocity vectors
β_j = payload ratio of jth stage $= p_j/W_{ji}$; $\bar{\beta}_j$ for no drag, Eq. (10)
γ = angle between velocity vector and horizontal
λ_j = propellant mass fraction for jth rocket motor
ξ = dimensionless time function, Eq. (11)
ξ_j, ξ'_j = dimensionless similarity parameters, Table 1
ρ_j = propellant density of jth stage, Eq. (18)

Received January 14, 1970; revision received March 2, 1970.
* Consultant. Member AIAA.

Subscripts

b,i = at burnout and ignition times, respectively
j,k = an arbitrary vehicle stage
m = a specific vehicle stage

Introduction

PAPERS addressing the problem of minimizing vehicle weight for specified payload and velocity at burnout generally either 1) permit a different specific impulse I for each stage,[1,2] but no provision for acceleration constraints, gravity, turning, or drag; or 2) provide for acceleration constraints and gravity,[3] but not for turning, different I's or drag. Reference 4, which maximizes payload total energy, does include acceleration constraints and the average effects of turning and I variation, but does not give an explicit formulation for determining these averages. In this Note, these formulations are included, as well as expressions for the average effects of drag for each stage. In addition, the angle between thrust and velocity vectors α will be considered in the aerodynamic sense (angle of attack) for those stages which include drag and as the angle for thrust vector control of the vehicle trajectory for those stages which neglect drag (exoatmospheric).

Formulation of the Problem

For a multistage vehicle whose trajectory is arbitrary and known from a computer solution, trajectory parameters can be established which isolate the weight and physical character of the rocket from the basic nature of the trajectory.[5] Such parameters will be used here to establish the average effects of drag, turning, angle of attack, and variation of I during burning. In Ref. 5, the equation of motion was taken in the direction of the body axis; here, the equation will be considered in the direction of the velocity vector:

$$F\cos\alpha - C_D qS - gW\sin\gamma/g_0 = W\dot{V}/g_0 \tag{1}$$

The thrust F and I are time varying and related by $F = -\dot{W}I$. Equation (1) can be written in the form

$$\dot{W} + GW = -JS \tag{2}$$

where $J = C_D q/(I\cos\alpha)$ and

$$G = \frac{\dot{V} + g\sin\gamma}{g_0 I\cos\alpha} = \frac{F\cos\alpha - C_D qS}{WI\cos\alpha} \tag{3}$$

Since the trajectory is known, J and G must be known functions of time, and Eq. (2) can be considered a first-order differential equation in W, the sea level vehicle weight. The solution to Eq. (2) for the jth stage is

$$W_{jb} = W_{ji}e^{-N_j} - Q_j S_j \tag{4}$$

where

$$N_j = N(t_{ji},t_{jb}) = \int_{t_{ji}}^{t_{jb}} G(t)dt \tag{5}$$

$$Q_j = Q(t_{ji},t_{jb}) = e^{-N_j}\int_{t_{ji}}^{t_{jb}} e^{N(t_{ji},t)}\, J(t)dt \tag{6}$$

The thrusting interval for the jth stage ($T_j = t_{jb} - t_{ji}$) must be selected so that $[1/(I\cos\alpha)]$ is defined for all t on this interval. If C_D is changed by a given percentage that is independent of Mach number, then Q_j will also change by this percentage. The $-\dot{W}_j(t)$ on the interval T_j is given by Eq. (9) of Ref. 5. The burnout value is

$$-\dot{W}_{ji} = G_j W_{ji} e^{-N_j} + (J_j - G_j Q_j)S_j \tag{7}$$

where G_j and J_j are at burnout.

Propellant and payload weights for the jth stage are related by

$$W_{jb} = p_j + (W_{ji} - p_j)(1 - \lambda_j) \tag{8}$$

With Eq. (4), this gives

$$p_j/W_{ji} \equiv \beta_j = \bar{\beta}_j/(1 + Q_j S_j/\lambda_j p_j) \tag{9}$$

where

$$\bar{\beta}_j = e^{-N_j}/\lambda_j - 1/R_j \tag{10}$$

and $R_j = \lambda_j/(1 - \lambda_j)$. When drag is neglected, $Q_j = 0$ and $\beta_j = \bar{\beta}_j$.

The over-all payload/gross-weight ratio is

$$p_n/W_{1i} = \prod_{j=1}^{n} \beta_j$$

The validity of this expression using the formulation of Eq. (9) for the inclusion of drag has been established for arbitrary trajectories (i.e., problem of Ref. 5). The problem is to determine the optimum set of v_j's which maximize p_n/W_{1i} subject to the constraint of a known V_t. It will be seen later that when drag is neglected, but gravity is not, the optimum acceleration for each stage is infinite; therefore, it is quite practical to constrain acceleration.

The propellant flow rate $(-\dot{W})$ is an arbitrary function of time and can be related to W_j and T_j by the dimensionless function $\xi(t)$. At burnout for the jth stage,

$$-\dot{W}_{jb} = \xi_j(W_{ji} - W_{jb})/T_j \tag{11}$$

From Eqs. (7–11),

$$T_j = \frac{\xi_j R_j(1 - \beta_j)}{G_j(1 + R_j\bar{\beta}_j) + (J_j/Q_j - G_j)(\bar{\beta}_j - \beta_j)R_j} \tag{12}$$

It is seen in Eq. (3) that $G_j I_j$ is closely related to the thrust-minus-drag to weight ratio at burnout. Therefore, the parameter G_j will be used as an acceleration constraint when gravity is not neglected. In Eq. (12), β_j approaches $\bar{\beta}_j$, and $(J_j/Q_j)(\bar{\beta}_j - \beta_j) \to 0$ as $Q_j \to 0$.

Approximations and Extremizing Equations

Equations (9), (12), and the p_n definition are exact expressions for relating the physical character of the vehicle to its arbitrary trajectory. We are looking for exact solutions when drag, angle of attack, and turning are neglected, and approximate solutions when these effects are included. A necessary approximation is

$$d\beta_j/dv_k = 0 \text{ for all } j \neq k \tag{13}$$

By multiplying

$$\sum_{j=1}^{n} v_j$$

by a Lagrangian multiplier and adding it to

$$\prod_{j=1}^{n} \beta_j,$$

the augmented function is obtained, and its change with respect to v_j (or v_k) must be zero; with the use of Eq. (13), the resulting extremizing equations are

$$(1/\beta_j)d\beta_j/dv_j = (1/\beta_k)d\beta_k/dv_k \tag{14}$$

where the Lagrangian multiplier has been eliminated between the jth and kth equations. Before this equation can be solved, we must eliminate S_j in Eq. (9), and obtain an approximate expression for N_j in Eq. (10).

From Eqs. (3) and (5), N_j can be considered as the sum of two integrals, A and B, where

$$A \equiv \int_{V_{ji}}^{V_{jt}} \frac{dV}{g_0 I\cos\alpha},\ B \equiv \int_{t_{ji}}^{t_{jb}} \frac{g\sin\gamma dt}{g_0 I\cos\alpha} \tag{15}$$

Since $v_j = V_{jb} - V_{ji}$ and $T_j = t_{jb} - t_{ji}$, average values will be defined by

$$1/C_j = A/v_j, \quad \bar{g}_j/C_j = B/T_j \tag{16}$$

The expression for N_j is now

$$N_j = A + B = (v_j + \bar{g}_jT_j)/C_j \tag{17}$$

where C_j and $\bar{g}_j$ estimate the average effects of exhaust gas velocity, gravity, angle of attack, and turning.

For the case of an end-burning solid-propellant, Eq. (14) of Ref. 5 is used:

$$S_j/p_j = \lambda_j(W_{ji}/p_j - 1)/(x_jT_j) \tag{18}$$

where $x_j = (1 - 2k_j)^2\rho_j\dot{r}_j$ and k_j is the average motor wall thickness per unit diameter (a known function of chamber pressure), ρ_j is the propellant weight density, and $\dot{r}_j$ is the linear burning rate. Equations (18) and (9) can be combined, yielding for a stage using an end-burning solid propellant;

$$\beta_j = (\bar{\beta}_j - \bar{Q}_j)/(1 - \bar{Q}_j), \quad \bar{Q}_j = Q_j/(x_jT_j) \tag{19}$$

For a given density and vehicle shape, the fineness ratio of a stage is proportional to $(W_{ji}/S_j)^{3/2}(W_{ji})^{1/2}$ and can be approximately constrained by constraining W_{ji}/S_j. Alternatively, $B_j \equiv W_{ji}/S_j$ can be considered as a ballistic coefficient at ignition. For the case where B_j is constant, Eq. (9) reduces to the form

$$\beta_j = \bar{\beta}_j - \bar{Q}_j, \quad \bar{Q}_j = Q_j/(\lambda_jB_j) \tag{20}$$

Other cases can, of course, be considered; e.g., constraining S_j/p_j in Eq. (9) results in a form quite similar to Eq. (19).

In the foregoing cases, β_j differs from that of no drag $(\beta_j = \bar{\beta}_j)$ by the single parameter $\bar{Q}_j$. If we assume $d\bar{Q}_j/dv_j \ll d\bar{\beta}_j/dv_j$, $d\bar{Q}_j/dv_j \simeq 0$, the solution to Eq. (14) is

$$\frac{1}{1 + \bar{\beta}_jR_j} = \left[1 - \frac{\bar{C}_m}{\bar{C}_j}\left(1 - \frac{1 + R_m\bar{Q}_m}{1 + R_m\bar{\beta}_j}\right)\right]\Big/(1 + R_j\bar{Q}_j) \tag{21}$$

where

$$1/\bar{C}_j = dN_j/dv_j = (1 + \bar{g}_jdT_j/dv_j)/C_j \tag{22}$$

Thus, $\bar{C}_j = C_j$ for those stages neglecting gravity; otherwise, $\bar{C}_j$ and $\bar{C}_m$ must be determined from Eq. (12). In Eq. (21), the subscript m is reserved for a particular stage for which a value of $\bar{\beta}_m$ will be chosen. With this value, and assuming $\bar{C}_j/\bar{C}_m$ is known, $\bar{\beta}_j$ is then determined for all j. However, it is necessary to see that V_t is also constrained. To do this, Eqs. (10) and (17) are combined to give

$$(C_j/C_m)\ln[(1 - \lambda_j)(1 + R_j\bar{\beta}_j)] = -(v_j + \bar{g}_jT_j)/C_m \tag{23}$$

By summing this equation on j, the result is

$$\sum_{j=1}^{n}\left[\frac{\bar{g}_jT_j}{C_m} + \frac{C_j}{C_m}\ln(1 + R_j\bar{\beta}_j)\right] = \frac{-V_t}{C_m} + \sum_{j=1}^{n}\frac{C_j}{C_m}\ln\frac{1}{1 - \lambda_j} \tag{24}$$

which is termed the compatibility equation. The right member of this equation is a known value, and a particular choice for $\bar{\beta}_m$ must result in a solution for T_j and $\bar{\beta}_j$ which satisfies this same value for the left member.

General Solution Including Drag

To obtain the expression for $\bar{C}_j$ in Eq. (22), the expression for T_j in Eq. (12) must first be determined, where β_j is given by Eq. (19) or (20). A general solution for T_j is obtained by writing Q_j as a function of $\bar{Q}_j$ from either Eq. (19) or (20) with the result

$$T_j = \{[\bar{\xi}_j(1 - \bar{\beta}_j) + \xi'_j]R_j\}/(G_jD_j - \bar{G}_jR_j/\lambda_j) \tag{25}$$

Table 1 Relations for $\bar{\xi}$, $\bar{G}$, and ξ'

	End-burning	Constant W_j/S_j	No drag
$\bar{\xi}$	$\xi - J/x$	ξ	ξ
$\bar{G}$	$G\bar{Q}$	$\lambda G\bar{Q} - J/B$	0
ξ'	0	$\xi\bar{Q}$	0

where $D_j = 1 + R_j\bar{\beta}_j$, and relations for $\bar{\xi}$, $\bar{G}$, and ξ' are given in Table 1. Keeping in mind that $d\bar{Q}_j/dv_j \simeq 0$, the solution for $\bar{C}_j$ can now be expressed as

$$\bar{C}_j = C_j[1 - d_jD_j/(D_j - b_j)^2] \tag{26}$$

where $b_j = \bar{G}_j/[G_j(1 - \lambda_j)]$ and

$$d_j = [\bar{g}_j\xi_j(1 - \bar{G}_j/G_j + \lambda_j\xi'_j/\bar{\xi}_j)]/C_jG_j(1 - \lambda_j) \tag{27}$$

Equation (21) can now be expressed as

$$(1 - h_j/D_j)[1 - d_jD_j/(D_j - b_j)^2] = L_mC_m/C_j \tag{28}$$

where $h_j = 1 + R_j\bar{Q}_j$, and

$$L_m = (1 - h_m/D_m)[1 - d_mD_m/(D_m - b_m)^2] \tag{29}$$

A convenient relation can now be written;

$$\bar{g}_jT_j = [C_jd_j - \bar{g}_j\bar{\xi}_j(D_j - b_j)]/(D_j - b_j) \tag{30}$$

From Eqs. (30) and (24), a compatibility function U can be defined

$$U = \sum_{j=1}^{n} u_j = \frac{-V_t}{C_m} + \sum_{j=1}^{n}\frac{C_j}{C_m}\left[\frac{\bar{g}_j\bar{\xi}_j}{C_jG_j} + \ln\frac{1}{1 - \lambda_j}\right] \tag{31}$$

where

$$u_j = (C_j/C_m)\,[\ln D_j + d_j/(D_j - b_j)] \tag{32}$$

Problems of this class are then solved as follows: 1) choose the mth stage and compute U from Eq. (31); 2) choose an L_m and compute all D_j from Eq. (28); and 3) compute all u_j from Eq. (32), and if $\Sigma u_j \neq U$, select a new L_m by use of a systematic process to effect convergence. The T_j's can then be determined from Eq. (30) and the v_j's from

$$v_j = -C_j\ln[D_j(1 - \lambda_j)] - \bar{g}_jT_j \tag{33}$$

Example problem 1

Consider the two-stage vehicle described as Design 2 in Table 1 of Ref. 5. The value for $\bar{K}$ in that table is in error and should read 272.71 psf. The V_t is 7035 fps, where the first stage will be constrained to the constant B_1 of 1507.5 lb/1.22 ft^2 = 1235.6 psf, and the second stage uses an end-burning solid-propellant motor with x_2 = 14.905 psf/sec. For this design, the values for G_1I_1 = 22.5 and G_2I_2 = 10.1, and the other parameter values are given in Table 2. The low value for $\bar{g}_2$ in this table is due to the turning of the sustainer vehicle off vertical. Since $C_1 = C_2$, the value for m can be either 1 or 2, and the compatibility function in Eq. (31) is determined as U = 2.50. It is seen in Table 2 that the initial values for u_j sum

Table 2 Initial values for example 1

Stage	1	2	Stage	1	2
Q_j, psf	2.318	72.74	λ_j	0.66	0.8955
J_j, psf/sec	5.373	0.0896	R_j	1.941	8.569
G_j, sec^{-1}	0.0994	0.04356	$\bar{Q}_j$	0.002841	0.09421
I_j, sec	226.2	232.7	h_f	1.0055	1.8073
$\bar{g}_j$, ft/sec^2	32.0	28.18	b_j	−0.1232	0.9015
$\bar{G}_j$, sec^{-1}	−0.004162	0.004104	d_j	0.1247	0.7677
T_j, sec	2.0	51.8	D_j	2.438	3.552
v_j, fps	1301	5734	$\bar{\beta}_j$	0.7406	0.2978
C_j, fps	7260	7260	β_j	0.7378	0.2248
ξ_j	1.0	1.0	u_j	0.94	1.56
$\bar{\xi}_j$	1.0	0.9940	L_j	0.56	0.28

Table 3 Final values for example 1

Stage	1	2	Stage	1	2
D_j	1.984	4.739	u_j	0.744	1.756
$\bar{\beta}_j$	0.5069	0.4363	T_j, sec	3.366	28.72
β_j	0.5041	0.3777	v_j, fps	2750	4290

to the correct value for U. However, the initial values for L_j are not equal to each other, but should be for an optimum design. Therefore, it is necessary to select new D_j's that give u_j's which still sum to $U = 2.50$, but which also have $L_1 = L_2 = L_m$ in Eq. (29). As a first estimate, choose L_m as the average of L_1 and L_2 (0.42) in Table 2, solve Eq. (28) for D_j and compute u_j from Eq. (32). This gives a value for U slightly different from the desired result. The correct value for L_m is 0.4658. The solution to Eq. (28) for $j = 1$ has only one real root for D_1; for $j = 2$ there are three real roots for D_2 with only the largest giving a positive value for β_2. Table 3 shows the optimized design with a new $p_n/W_{1i} = \beta_1\beta_2$ 13% larger than that of the initial design. Although G_2I_2 has not changed, G_1I_1 (with a new $S_1 = 1.06$ ft^2 and $v_1 = 2750$ fps) is 26.4 instead of 22.5.

Solution Neglecting Drag

With the use of Table 1, the previous section can be used for cases where drag must be included for some stages but can be neglected for others. If drag is neglected for all stages, the solution can be described graphically for any number of stages. Equation (28) becomes

$$(1 - 1/D_j)(1 - d_j/D_j) = L_m C_m / C_j \tag{34}$$

where $L_m = (1 - d_m/D_m)(1 - 1/D_m)$. Equation (30) can be written as

$$\bar{g}_j T_j = d_j C_j (\lambda_j - 1 + 1/D_j) \tag{35}$$

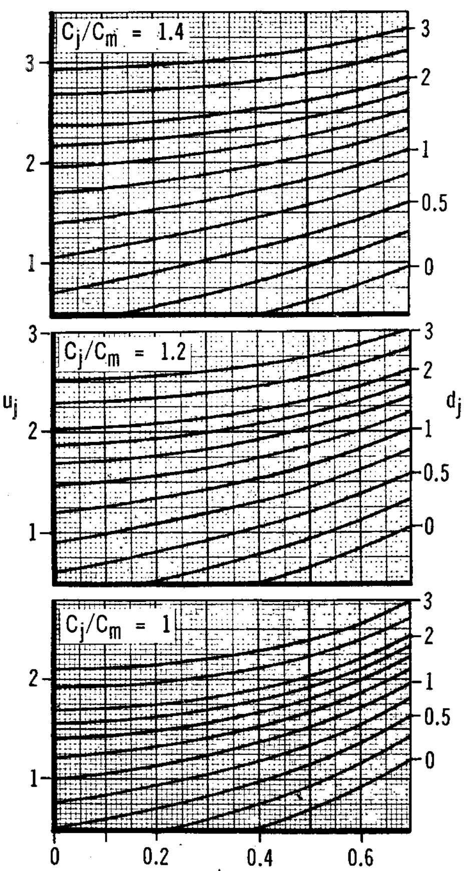

Fig. 1 u_j **vs** L_m **for various** d_j **and** C_j/C_m.

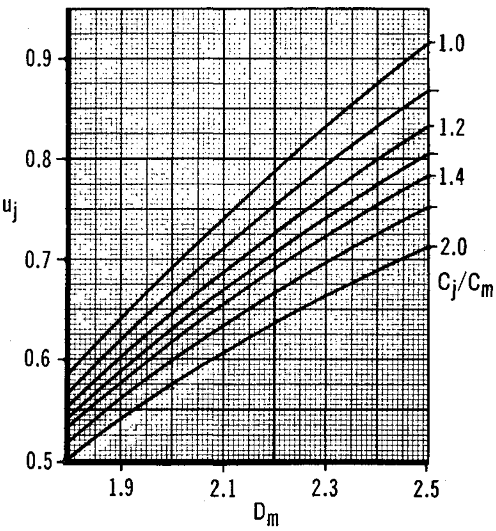

Fig. 2 u_j **vs** D_m **for various** C_j/C_m.

and the compatibility function becomes

$$U = \sum_{j=1}^{n} u_j = \frac{-V_t}{C_m} + \sum_{j=1}^{n} \frac{C_j}{C_m}\left[d_j(1 - \lambda_j) + \ln\frac{1}{1 - \lambda_j}\right] \tag{36}$$

where

$$u_j = (C_j/C_m)(d_j/D_j + \ln D_j) \tag{37}$$

It is not required that all d_j be finite; $\bar{g}_j$ may be zero either from neglecting gravity or from horizontal flight. For this case, the solution to Eq. (34) is

$$D_j = 1/(1 - L_m C_m/C_j), \quad d_j = 0 \tag{38}$$

For $d_j \neq 0$, Eq. (34) is a quadratic in D_j, and the largest root, corresponding to the largest β_j, for a fixed u_j in Eq. (37) is

$$\frac{1}{D_j} = 1 - \left(\frac{d_j - 1}{2d_j}\right) - \left[\left(\frac{d_j - 1}{2d_j}\right)^2 + \frac{C_m}{C_j}\frac{L_m}{d_j}\right]^{1/2} \tag{39}$$

where L_m must not be negative. If there exists a negative L_m for a given u_j, then there also exists a positive L_m with a larger β_j. Furthermore, for $d_j > 1$, $D_j \geq d_j$ and $u_j \geq (C_j/C_m)(1 + \ln d_j)$ for an optimum solution. For $d_j < 1$, the minimum D_j is unity and the minimum u_j is $(C_j/C_m)d_j$. If these minimum u_j's are substituted into Eq. (36), the solution for V_t is the maximum permissible value for given d_j's, λ_j's, and C_j's.

Figure 1 shows u_j vs L_m for various values of d_j and C_j/C_m. Any problem of this class can be solved quickly by first determining the compatibility function U from Eq. (36) and then finding one value for L_m in Fig. 1 such that the values for u_j sum to U. This reduces the iterative process to a simple summing of numbers. All D_j and payload ratios $\beta_j = (D_j - 1)/R_j$ are determined by Eqs. (38) or (39), and all T_j from (35). The v_j's are then found by Eq. (33).

Example problem 2

Consider the problem of Schurmann[3] for a 3-stage vehicle with $V_t = 25{,}000$ fps and G_jI_j of 8, 10, and 8, respectively, where $I_j = 300$ sec constant for each stage. Since the value for G_j is the thrust-to-weight ratio divided by I_j, and $C_j = g_0 I_j$, the values for d_j in Eq. (27) are 2.5, 2, and 1.25, respectively, where all $\xi_j = 1$, all $\bar{g}_j = g_0$, and the λ_j's are 0.95, 0.95, and 0.90, respectively. From Eq. (36), $U = 6.054$. We need to find an L_m in Fig. 1 such that the u_j's in Eq. (37) sum to 6.054. A first estimate for L_m of 0.5 is obtained from the bottom graph in Fig. 1 at the point corresponding to the average u_j (i.e., $U/3$) $\simeq 2$ and the average $d_j \simeq 1.9$. The correct value is $L_m = 0.5253$. From Eq. (39), the D_j's are 6.571, 5.562, and 4.097, respectively, and the values for $\beta_j = (D_j - 1)/R_j$ are 0.2933, 0.2401, and 0.3441, respectively. From Eq. (35), $T_1 = 76.64$ sec, $T_2 = 77.88$ sec, and $T_3 = 54.04$ sec. From Eq. (33) $v_1 = 8278$ fps, $v_2 = 9847$, and $v_3 = 6875$. Of course, the method presented here, unlike the method of Schurmann,[3] provides for cases in which the I_j's differ.

Solution Neglecting Drag and Gravity

When gravity is neglected for all stages, $d_j = 0$ and Eq. (34) becomes

$$D_j = D_m/[D_m - (D_m - 1)C_m/C_j] \tag{40}$$

The u_j's are given by Eq. (37) where $d_j = 0$, and U by Eq. (36). Figure 2 can be used to solve all problems of this class. One simply has to find a D_m in Fig. 2 such that the u_j's sum to U.

Example problem 3

Consider a 4-stage rocket with values for C_j/g_0 of 250, 275, 300, and 325 sec, respectively, with λ_j's of 0.9, 0.85, 0.8, and 0.75, respectively, and with $V_t = 40{,}000$ fps. We choose $m = 1$, and the values for C_j/C_m become 1, 1.1, 1.2, and 1.3, respectively, and U is determined to be 3.14 from Eq. (36). A first estimate for D_m of 2.32 is obtained from Fig. 2 at the point corresponding to the average u_j (i.e., $U/4$) and the average C_j/C_m. The correct solution for D_m in Fig. 2 with u_j's which sum to $U = 3.14$ is 2.31. The values for D_j are now determined from Eq. (40) and from $\bar{\beta}_j = \beta_j = (D_j - 1)/R_j$, the β_j's are 0.1455, 0.189, 0.224, and 0.258, respectively. The v_j's are determined from Eq. (33) with $\bar{g}_j = 0$, and $p_n/W_{1_i} = 1/630$.

References

[1] Subotowicz, M., "The Optimization of the N-Step Rocket with Different Construction Parameters and Propellant Specific Impulses in Each Stage," *Jet Propulsion,* Vol. 28, No. 7, July 1958, pp. 460–463.

[2] Hall, H. H. and Zambelli, E. D., "On the Optimization of Multistage Rockets," *Jet Propulsion,* Vol. 28, No. 7, July 1958, pp. 463–365.

[3] Schurmann, E. E. H., "Optimum Staging for Multistaged Rocket Vehicles," *Jet Propulsion,* Vol. 27, No. 8, Pt. 1, Aug. 1957, pp. 863–865.

[4] Cobb, E. R., "Optimum Staging Technique to Maximize Payload Total Energy," *ARS Journal,* Vol. 31, No. 3, March 1961, pp. 342–344.

[5] Adkins, C. N., "Rocket Design for a Specified Trajectory," *Journal of Spacecraft and Rockets,* Vol. 2, No. 2, March-April 1965, pp. 249–253.

A Schlieren Technique for Measuring Jet Penetration into a Supersonic Stream

Martin Hersch,* Louis A. Povinelli,†
and Frederick P. Povinelli*
NASA Lewis Research Center, Cleveland, Ohio

Introduction

JET penetration into a supersonic stream may be determined from concentration measurements (Refs. 1–5), or more readily from schlieren photographs (Refs. 4 and 6).

Received January 23, 1970; revision received February 24, 1970.

* Aerospace Research Engineer.

† Research Scientist. Associate Fellow AIAA.

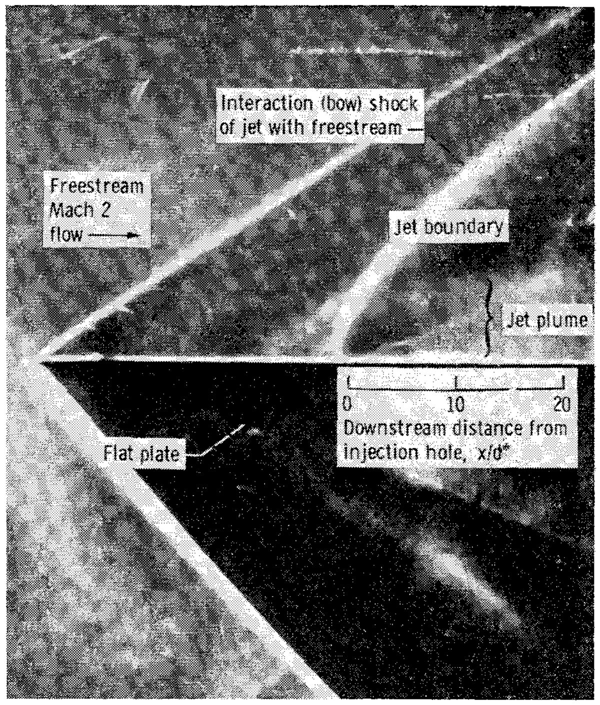

Fig. 1 Typical schlieren photograph (negative). Injection Mach number, 1.0; injection pressure, 100 psia (6.89×10^5 N/m²).

The essential features of the jet flowfield, as seen on a schlieren photograph, are diagramed in Fig. 1. Schetz, Hawkins, and Lehman[6] used the location of the center of the Mach disk as a measure of jet penetration. Zukoski and Spaid[4] used the upper portion of the shock structure as a criterion of penetration. The jet shock structure is located close to the injection orifice. Therefore, penetration measurements based on location of the jet shock structure may not completely describe the downstream behavior of the jet. Furthermore, it appears that for some injectants or operating conditions, the jet shock structure is difficult to detect, or may even be completely invisible. An alternate optical method for measuring jet penetration is thus desirable. In this study it is noted that the path of a helium jet may be detected by schlieren photography. The jet appeared as a plume shaped streak in the flowfield, as shown in Fig. 1. Measurements of helium jet penetration into a Mach 2 airstream were made by densitometer analysis and visual inspection of schlieren photographs and compared to results based on concentration measurements.

Helium was injected from a flat plate into a Mach 2 airstream. The injection was normal to the freestream, and injection Mach numbers were 1, 2.4, 3.5, and 4. The injection total pressure was varied from 48 psia (3.30×10^5 N/M^2) to 130 psia (8.96×10^5 N/M^2). The injection throat diameter for all injection conditions was 1.9 mm. Freestream total pressure and temperature were 0.92 atm (9.3×10^4 N/M^2), and 625°R (347°K).

Fig. 2 Jet flowfield.